Nonuniform Traffic Distribution Model in Reverse Link of Multirate/Multiservice WCDMA-Based Systems

Ferran Adelantado, *Student Member, IEEE*, Jordi Pérez-Romero, *Member, IEEE*, and Oriol Sallent

***Abstract*—This paper focuses on the modeling of the reverse link of a wideband code division multiple access system in a nonhomogeneous environment with a single cell. Multiple traffic spatial and service nonuniformities are considered in the analytical model, and then, expressions for required transmitted power and the associated outage probability and block error rate are derived. Special attention is also paid to the effect caused by different transmission bit rates and the spatial location of the traffic nonuniformities. From the presented expressions, it is possible to set appropriate load thresholds to control the desired error rate. Although the model considers a single cell, results in terms of maximum allowable load can also be applicable in multicell scenarios.**

***Index Terms*—Load factor, nonuniformities, service distribution, traffic distribution, wideband code division multiple access (WCDMA) capacity.**

I. Introduction

ONE of the main traffic characteristics in cellular networks is nonhomogeneous traffic spatial distribution. To cope with this inherent aspect in mobile communication scenarios, system deployment must be preceded by careful network planning. Network planning takes into account the expected traffic load all over the service area in order to come up with a solution on how many base stations are required and what are the suitable locations to set up the sites. Certain operator's objectives in coverage, capacity, and quality must be met in the planning exercise. Furthermore, in the context of multimedia services, traffic needs to be detailed also in terms of traffic class spatial distribution (e.g., expected conversational traffic and interactive traffic) because of the different quality of service (QoS) requirements.

Nevertheless, although network planning can consider these nonhomogeneities at some extent, the high dynamics associated with the traffic generation processes coupled with user mobility clearly need additional mechanisms to cope with the potential problems with network performance derived from traffic profile distributions that are significantly different from those expected in the network planning phase. Traffic level and service mix variations along time and space, thus resulting in different load levels in different cells and times, may result in an observed QoS that is significantly different from the planned values, hence negatively impacting the user's mobile experience.

In the context of wideband code division multiple access (WCDMA) systems, service and traffic spatial distributions become even more important, since there is a tight dependence of the interference level observed on every user's position in the network and the corresponding transmitted power levels. Clearly, the research community has already targeted these aspects. First approaches may be found in [1] and [2], where the impact of certain traffic distributions is analyzed by simulations and analytical expressions. This paper is focused on the characterization of the effect of nonuniformities in the reverse link of a WCDMA system. Thus, the major difference with respect to [1] and [2] lies in the fact that in these papers, no service mix is considered, and therefore, only specific traffic spatial distributions are analyzed. On the contrary, this paper presents an accurate traffic description that allows the specification of a generic scenario by breaking it down into different traffic layers, and therefore, general expressions for spatial distributions are obtained. Moreover, each layer is associated with a specific and independent service distribution. Required power expressions that have been obtained are general, and thus, they can be applied to any scenario regardless of the number of layers it consists of. This paper is an evolution of a previous work [3], where simulations showed that nonuniformities meant a new challenge to be faced in terms of capacity and a scenario with a single hotspot was analyzed by simulations. In this context, the formulation of the general problem is developed throughout this paper.

Other approaches presented in the literature also cope with techniques to mitigate the effects caused by nonuniformities. Radio resource management (RRM) strategies have become one of the targets [4], specifically call admission control (CAC) and load control, on which many studies have been carried out. In [5] and [6], different algorithms are presented and simulated, achieving positive results in maximizing the capacity while minimizing parameters such as blocking probability. Finally, pilot power management has also emerged as a solution to balance the load among base stations in nonhomogeneous scenarios. For instance, in [7]–[11], different algorithms are proposed, and all of them focused on forward link. In this respect,

Manuscript received December 19, 2005; revised July 19, 2006, October 10, 2006, and November 29, 2006. This work was supported in part by the European Community and in part by the Spanish Research Council (CICYT) under COSMOS Grant (Ref. TEC2004-00518, Spanish Ministry of Science and Education and European Regional Development Fund). The review of this paper was coordinated by Dr. W. Zhuang.

The authors are with the Universitat Politècnica de Catalunya, 08034 Barcelona, Spain.

Digital Object Identifier 10.1109/TVT.2007.900386

this paper may also serve as the basis for further development of these RRM techniques (e.g., devising admission and congestion thresholds), as long as the analytical approach allows us to gain insight into the general problem. RRM and CAC, in particular, are of crucial importance for the correct behavior of the system. The limitation of the interference lies on this mechanism and allows guaranteeing a maximum load level that should not be exceeded. These load thresholds must be determined by taking into account aspects such as the service used by users, their activity factor, and their spatial distribution. In fact, their huge variability is shown in this paper.

As aforementioned, this paper focuses on modeling traffic nonhomogeneities from an analytical perspective, so that the key issues affecting the problem can be extracted. The final objective is to propose a model able to compute the maximum capacity (i.e., maximum uplink load factor) that can be supported in the uplink of a WCDMA cell under nonhomogeneous spatial traffic distribution and multiple services. This maximum load factor value can then be used as an input to dynamic RRM strategies, e.g., admission or load control. Capacity will be defined for specific outage probability requirements. The analytical expressions have been derived for a single cell model. However, as it will be discussed in this paper, results in terms of maximum load factor could also be applicable in a multicell scenario. Additionally, the envisaged impact of soft handover is discussed. The remainder of this paper is organized as follows: The problem formulation is presented in Section II. Section III proposes a model for computing the transmitted power distribution in nonuniformly distributed scenarios and derives outage probability. Finally, Section IV presents results for some representative case studies, and Section V presents the conclusions.

II. Problem Formulation

The considered scenario is an isolated WCDMA cell with radius R (in meters). This scenario is composed of N overlapped layers (L_i, with $0 \leq i \leq N-1$), each one with specific traffic and service characteristics. All layers are circular shaped with a radius r_i (in meters) and their center is placed D_i (in meters) from the cell site. In particular, layer L_0 matches up with the cell area, and thus, $D_0 = 0$ and $r_0 = R$ (the cell site is set as the coordinate origin). The scenario layout is shown in Fig. 1.

Let us denote T_T as the total number of users within the cell. T_T is distributed among the N layers, and the proportion of users belonging to layer L_i is given by

$$\alpha_i = \frac{T_i}{\sum_{j=0}^{K-1} T_j} = \frac{T_i}{T_T} \tag{1}$$

where T_i is the number of users within layer L_i. On the other hand, K possible services ($0 \leq n \leq K-1$) are identified. $\rho_{i,n}$ denotes the proportion of users with the nth service in layer L_i. In general, the traffic source is not continuously transmitting packets within a session, and some activity periods alternate with inactivity periods (e.g., reading time during a World Wide Web download or silence periods in speech calls). Then, the

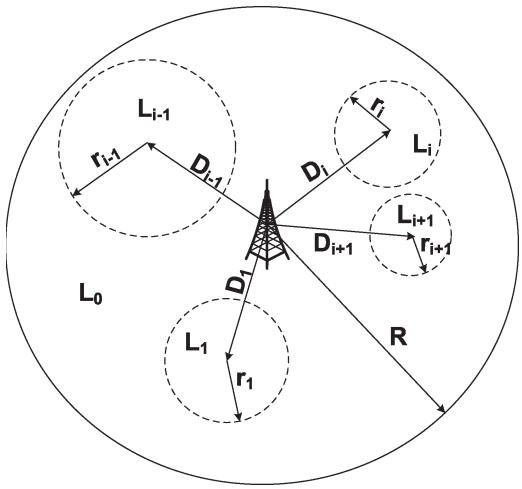

Fig. 1. Scenario layout.

activity factor for the nth service (ϵ_n) is defined as the proportion of time in which a user is transmitting for this service, taking into account session and intersession times.

With respect to activity periods in which a certain user is transmitting data through the air interface, there may exist several possibilities for each service to transmit the data flow, which is characterized essentially by a transmission bit rate, a channel code, and a required E_b/N_0. Following the Third Generation Partnership Project (3GPP) terminology [13], these possibilities will be denoted as a transport format (TF, hereafter).[1] Each TF is characterized by a transmission bit rate and an E_b/N_0 target. Then, the set of TFs is denoted as a TF set (TFS). In particular, TFS_n stands for the TFS of the nth service. The set of possible bit rates for the nth service is $R_{b_{n,j}} (0 \leq j \leq \text{TFS}_n - 1)$, and the corresponding E_b/N_0 is $(E_b/N_0)_{n,j}$ with $0 \leq j \leq \text{TFS}_n - 1$. $p_{n,j}$ is defined as the probability that the nth service uses the jth TF, which depends on the specific medium access control (MAC) algorithm that executes the TF selection in the uplink (see, e.g., [4] with some examples).

In Section III, an analytical model of the reverse link of a multirate/multiservice WCDMA-based system is developed. The main target of this paper is to obtain a model to study the impact of nonuniformities on the performance of the system. The QoS parameters under study are the outage probability, which is defined as the probability that the measured $(E_b/N_0)_m$ is below the target, and the block error rate (BLER), which is defined as the percentage of erroneous blocks received by the base station. Notice that outage and BLER are tightly coupled with transmitted power, and thus, the study of the transmitted power becomes the key issue.

The process carried out in Sections III-A and B is aimed at determining the required transmitted power probability density function (pdf) expression to evaluate the outage probability and BLER performance.

[1] Notice that, although the 3GPP terminology is used here, the concept of TF would be general to any code division multiple access system with variable transmission bit rate.

III. Analytical Model

A. Transmitted Power Distribution

In WCDMA-based systems, the capacity is highly dependent on the interference existing in the air interface. The main goal of this section is to determine the expression of the required transmitted power pdf to derive the system capacity. In the uplink case, the required transmitted power (in logarithmic units) is given by [4]

$$P(\text{dBm}) = Z\ (\text{dB}) + 10\ \log\left(\frac{P_N}{(1-\eta)\left(\frac{W}{\left(\frac{E_b}{N_0}\right)R_b}+1\right)}\right) = Z + \Phi \tag{2}$$

where W is the total bandwidth after spreading, P_N is the thermal noise power, Z is the total propagation loss (path loss plus a shadowing component), E_b/N_0 is the target energy per bit versus interference plus noise spectral density, and η is the uplink load factor [3]. The load factor is defined as the proportion of the power generated by users (own-cell power and other-cells interference) with respect to the total power (thermal noise power, own-cell received power, and other-cell interference), and thus, it is tightly coupled with the maximum number of users that can be allocated in the cell (the maximum cell capacity), i.e.,

$$\eta = \frac{P_R + P_I}{P_N + P_R + P_I} = 1 - \frac{P_N}{P_N + P_R + P_I} \tag{3}$$

where P_R is the total own-cell received power, and P_I is the total other-cell interference. Particularizing (3) for a single cell scenario, the load factor is given by

$$\eta = \frac{P_R}{P_N + P_R} = 1 - \frac{P_N}{P_N + P_R}. \tag{4}$$

In general, RRM algorithms in the uplink tend to control the load factor. Thus, the presented model intends to determine the maximum admissible load factor on the basis of traffic distribution and desired quality.

For a given load factor η, the required transmitted power becomes a function of total loss, E_b/N_0, and R_b. Thus, the required transmitted power (P) pdf may be obtained by calculating the pdf of the total loss Z, which depends on traffic spatial distribution, and of the product $(E_b/N_0)\cdot R_b$, which depends on service characterization. The total propagation loss is defined as

$$Z(\text{dB}) = Y(\text{dB}) + S(\text{dB}) \tag{5}$$

where Y is the path loss dependent on the distance, and S is the lognormal shadowing component (assuming that closed-loop power control cancels all fast fading effects). The path loss at distance d (in meters) from the transmitter in logarithmic units Y (in decibels) is typically given by

$$Y(\text{dB}) = Y_0 + \zeta \log d \tag{6}$$

where Y_0 and ζ are constants and depend on the environment. Then, the path loss distribution is determined by the traffic spatial distribution (i.e., the distribution of the distance d). Focusing on a generic layer L_i (characterized by its radius r_i and the distance D_i from the cell site to its center), the path loss pdf, which is denoted as $f_Y^i(y)$, is given as follows (see the Appendix for details):

if $D_i \geq r_i$:

$$f_Y^i(y) = \frac{A\beta}{2\pi r_i^2} e^{\beta y}\left[\pi - 2\arcsin\frac{D_i^2 - r_i^2 + Ae^{\beta y}}{2D_i\sqrt{(A)}e^{\beta\frac{y}{2}}}\right] \tag{7}$$

in the range $Y_0 + \zeta\log(D_i - r_i) \leq y \leq Y_0 + \zeta\log(D_i + r_i)$;

if $D_i < r_i$:

$$f_Y^i(y) = \frac{A\beta}{r_i^2} e^{\beta y} \tag{8}$$

in the range $-\infty < y \leq Y_0 + \zeta\log(r_i - D_i)$; and

$$f_Y^i(y) = \frac{A\beta}{2\pi r_i^2} e^{\beta y}\left[\pi - 2\arcsin\frac{D_i^2 - r_i^2 + Ae^{\beta y}}{2D_i\sqrt{(A)}e^{\beta\frac{y}{2}}}\right] \tag{9}$$

in the range $Y_0 + \zeta\log(r_i - D_i) < y \leq Y_0 + \zeta\log(D_i + r_i)$, where $A = 10^{-2(Y_0/\zeta)}$, and $\beta = 2(\ln(10)/\zeta)$.

Adding the effects of lognormal shadowing S, the total propagation loss $(Z = Y + S)$ pdf is the result of convolutioning (7)–(9) and a Gaussian function with null mean and σ^2 variance, so that the resulting pdf can be expressed as

$$f_Z^i(z) = f_Y^i(z) * \frac{1}{\sqrt{2\pi}\sigma} e^{-\frac{z^2}{2\sigma^2}} \tag{10}$$

where $*$ denotes the convolutional operator.

Finally, the overall total propagation loss density function is obtained by summing each pdf that is weighted according to the traffic fraction α_i of each layer. In particular, when N layers are considered (from 0 to $N-1$), the final total propagation loss density function is given by

$$f_Z(z) = \sum_{i=0}^{N-1} \alpha_i f_Z^i(z). \tag{11}$$

It may be observed from (2) that the required transmitted power is also dependent on Φ. In the case of WCDMA-based systems, only transmitting users (i.e., during activity periods) contribute to an increase of the interference. Taking this fact into account, the influence of each user on the total interference depends on the activity factor ϵ_n, the services, the selected TF, and the distribution of services within the layers $(\rho_{i,n})$.

Therefore, Φ is a random variable whose probability function is given by

$$P_\Phi(\Phi = \phi_{n,j}) = \sum_{i=0}^{N-1} P_\Phi^i(\phi_{n,j}) \tag{12}$$

where P_Φ^i is given as follows:

$$P_\Phi^i(\phi_{n,j}) = \frac{\beta_n \alpha_i \rho_{i,n} p_{n,j}}{\sum_{s=0}^{K-1}\sum_{q=0}^{N-1} \alpha_q \beta s \rho_{q,s}} \tag{13}$$

and $\phi_{n,j}$ is defined as

$$\phi_{n,j} = 10\log\left(\frac{P_N}{(1-\eta)\left(\frac{W}{\left(\frac{E_b}{N_0}\right)_{n,j} R_{b_{n,j}}} + 1\right)}\right) \tag{14}$$

for $j = 0, \ldots, \text{TFS}_n - 1$. Thus, (13) is defined in a discrete probability space $\Omega_\Phi = \{\phi_{0,0}, \phi_{0,1}, \ldots, \phi_{K-1,\text{TFS}_{K-1}-1}\}$.

Finally, from (2), for a given load factor the required transmitted power pdf is obtained by convolutioning Z and Φ pdfs, i.e.,

$$f_P(P) = f_Z(P) * f_\Phi(P). \tag{15}$$

Therefore, by combining (11) and (13), the required transmitted power density function results in

$$f_P(P) = \frac{\sum_{n=0}^{K-1}\sum_{j=0}^{TFS_n-1}\sum_{i=0}^{N-1} \alpha_i \epsilon_n \rho_{i,n} p_{n,j} f_Z^i(P - \phi_{n,j})}{\sum_{s=0}^{K-1}\sum_{q=0}^{N-1} \alpha_q \epsilon_s \rho_{q,s}}. \tag{16}$$

The required transmitted power pdf may be obtained by the following expressions for each layer and service, respectively:

$$f_P^i(P) = \frac{\sum_{n=0}^{K-1}\sum_{j=0}^{TFS_n-1} \epsilon_n \rho_{i,n} p_{n,j} f_Z^i(P - \phi_{n,j})}{\sum_{s=0}^{K-1} \epsilon_s \rho_{i,s}} \tag{17}$$

$$f_{Pn}(P) = \frac{\sum_{i=0}^{N-1}\sum_{j=0}^{TFS_n-1} \alpha_i \rho_{i,n} p_{n,j} f_Z^i(P - \phi_{n,j})}{\sum_{i=0}^{N-1} \alpha_i \rho_{i,n}}. \tag{18}$$

Notice that no power limitations have been taken into account so far. In real user equipment, transmitted power in the reverse link will be limited by an upper threshold (P_{Tmax}) and a lower threshold (P_{Tmin}). Then, the modified transmitted power distribution taking into account power constraints ($f_P^*(P)$) will be given by

$$f_P^*(P) = \begin{cases} 0, & P < P_{\text{Tmin}} \\ \int_{-\infty}^{P_{\text{Tmin}}} f_P(P)dP, & P = P_{\text{Tmin}} \\ f_P(P), & P_{\text{Tmin}} < P < P_{\text{Tmax}} \\ \int_{P_{\text{Tmax}}}^{\infty} f_P(P)dP, & P = P_{\text{Tmax}} \\ 0, & P > P_{\text{Tmax}} \end{cases}. \tag{19}$$

B. QoS Evaluation

This section extracts from the previous model the QoS performance in terms of outage probability μ and BLER. It is assumed as an ideal power control so that the transmitted power is the required one, provided that it is between the limit $[P_{\text{Tmin}}, P_{\text{Tmax}}]$. A user is said to be in outage whenever the measured $(E_b/N_0)_m$ is below the target value E_b/N_0 or equivalently when P is above P_{Tmax}. Then, the outage probability μ may be expressed as

$$\begin{aligned} \mu &= prob\left(\left(\frac{E_b}{N_0}\right)_m < \left(\frac{E_b}{N_0}\right)\right) \\ &= prob(P > P_{\text{Tmax}}). \end{aligned} \tag{20}$$

For a given load factor, the outage probability expression is given as follows:

$$\mu_\eta = \int_{P_{\text{Tmax}}}^{\infty} f_P(P)dP \tag{21}$$

$$\mu_\eta = \frac{\sum_{n=0}^{K-1}\sum_{j=0}^{TFS_n-1}\sum_{i=0}^{N-1} \alpha_i \epsilon_n \rho_{i,n} p_{n,j} \lambda_{i,n,j}}{\sum_{s=0}^{K-1} \epsilon_s \sum_{q=0}^{N-1} \alpha_q \rho_{q,s}} \tag{22}$$

with

$$\lambda_{i,n,j} = \int_{P_{\text{Tmax}}}^{\infty} f_Z^i(P - \phi_{n,j})dP. \tag{23}$$

Likewise, BLER depicts the percentage of erroneous transport blocks (TB) received by the base station. TB is the minimum amount of information that can be exchanged between the physical and MAC layers. It includes a data part and the MAC and radio link control headers. BLER, which is given in the following expression, is a function of $(E_b/N_0)_m$ and depends on physical layer aspects such as channel coding, modulation, and interleaving:

$$\text{BLER} = b_{n,j}\left(\left(\frac{E_b}{N_0}\right)_m\right) \tag{24}$$

where the function $b_{n,j}(\cdot)$ is specific for each service and TF.

Whenever the required power P is between P_{Tmax} and P_{Tmin}, the user will be able to reach the target E_b/N_0, so that $E_b/N_0 = (E_b/N_0)_m$. On the contrary, when the required

power P is above the maximum available P_{Tmax}, the measured $(E_b/N_0)_m$ is lower than the target E_b/N_0. In particular, $(E_b/N_0)_m$ will be $(P - P_{\mathrm{Tmax}})$ dB below the target E_b/N_0. On the contrary, when P is below P_{Tmin}, the difference between $(E_b/N_0)_m$ and E_b/N_0 is equal to $P_{\mathrm{Tmin}} - P$, and in this case, the measured $(E_b/N_0)_m$ is above the target.

Summarizing these situations, the measured $(E_b/N_0)_m$ as a function of the required transmitted power P is given by

$$\left(\frac{E_b}{N_0}\right)_m = g(P) = \begin{cases} \left(\frac{E_b}{N_0}\right)\frac{P_{\mathrm{Tmin}}}{P}, & P < P_{\mathrm{Tmin}} \\ \left(\frac{E_b}{N_0}\right), & P_{\mathrm{Tmin}} \le P \le P_{\mathrm{Tmax}} \\ \left(\frac{E_b}{N_0}\right)\frac{P_{\mathrm{Tmax}}}{P}, & P > P_{\mathrm{Tmax}} \end{cases}. \tag{25}$$

Therefore, BLER is a function of the required transmitted power, i.e.,

$$\mathrm{BLER} = \gamma_{n,j}\left(g(P)\right) = \gamma_{n,j}(P) \tag{26}$$

where $\gamma_{n,j}(\cdot)$ is the function relating BLER and transmitted power for service n and TF j. In particular, for a given load factor, BLER is given as follows:

$$\overline{\mathrm{BLER}_\eta} = \int_{-\infty}^{\infty} \gamma(P) f_P(P) dP \tag{27}$$

$$\overline{\mathrm{BLER}_\eta} = \frac{\sum_{n=0}^{K-1}\sum_{j=0}^{TFS_n-1}\sum_{i=0}^{N-1}\alpha_i\epsilon_n\rho_{i,n}p_{n,j}\vartheta_{i,n,j}}{\sum_{s=0}^{K-1}\epsilon_s\sum_{q=0}^{N-1}\alpha_q\rho_{q,s}} \tag{28}$$

with

$$\vartheta_{i,n,j} = \int_{-\infty}^{\infty} \gamma_{n,j}(P) f_Z^i(P - \phi_{n,j}) dP. \tag{29}$$

In turn, the outage probability and BLER for a specific layer [(30) and (32)] or service [(31) and (33)] are shown as follows:

$$\overline{\mathrm{BLER}_\eta^i} = \frac{\sum_{n=0}^{K-1}\sum_{j=0}^{TFS_n-1}\epsilon_n\rho_{i,n}p_{n,j}\vartheta_{i,n,j}}{\sum_{s=0}^{K-1}\epsilon_s\rho_{i,s}} \tag{30}$$

$$\overline{\mathrm{BLER}_{\eta,n}} = \frac{\sum_{i=0}^{N-1}\sum_{j=0}^{\mathrm{TFS_n}-1}\alpha_i\rho_{i,n}p_{n,j}\vartheta_{i,n,j}}{\sum_{i=0}^{N-1}\alpha_i\rho_{i,n}} \tag{31}$$

$$\mu_\eta^i = \frac{\sum_{n=0}^{K-1}\sum_{j=0}^{TFS_n-1}\epsilon_n\rho_{i,n}p_{n,j}\lambda_{i,n,j}}{\sum_{s=0}^{K-1}\epsilon_s\rho_{i,s}} \tag{32}$$

$$\mu_{\eta,n} = \frac{\sum_{i=0}^{N-1}\sum_{j=0}^{TFS_n-1}\alpha_i\rho_{i,n}p_{n,j}\lambda_{i,n,j}}{\sum_{i=0}^{N-1}\alpha_i\rho_{i,n}}. \tag{33}$$

Notice that (30)–(33) relate the performance in terms of outage probability and BLER with a specific value of the load factor. Consequently, they allow obtaining the maximum load factor that ensures the desired performance constraints (i.e., the maximum BLER or the maximum outage probability). It is worth mentioning that this maximum load factor establishes the maximum total interference level allowed in the cell, regardless of how it is distributed between intercell or intracell interference. Therefore, although the model considers a single cell (i.e., the cell under study), the maximum obtained load factor would also be applicable in a multicell scenario (i.e., in such a case, the total maximum interference allowed in the cell would be the same, but depending on the scenario, the specific value of inter- or intracell interference could be different).

It is worth noting that all the expressions developed so far have been obtained by considering circular layers. However, the methodology would also be applicable to any other shape if propagation loss density functions are known. It is also remarkable that, for instance, it is possible to follow the same process if a measurement campaign is carried out and there is a previous knowledge of the area that is to be analyzed in terms of total propagation loss distribution. Similarly, if soft handover was to be included, this would basically modify the path loss of the users of the cell under study in (10) because it would be possible that some users located in other cells were connected to the cell under study, while the rest of the procedure would basically be the same.

IV. Results

This section presents three relevant examples in order to provide insight on the proposed model and to illustrate its capabilities under different traffic and service distributions. In addition, the validation of the model through simulations is given. All results have been obtained considering the propagation model exposed in (6) plus a lognormal shadowing. In particular, the parameters have been set to $Y_0 = 128.1$, $\zeta = 37.6$, $\sigma = 3$ dB, $P_N = -103$ dBm, $P_{\mathrm{Tmax}} = 21$ dBm, and $P_{\mathrm{Tmin}} = -44$ dBm. Two services (service 0 and service 1) are considered. Service parameters are detailed in Table I. Service 0 intends to represent a conversational case-based reasoning service that generates traffic at 64 kb/s. On the other hand, service 1 intends to represent an interactive service with four possible transmission bit rates. This makes the selection of a transmission bit rate a key issue in terms of the generated interference and QoS parameters such as outage probability and BLER. The physical layer has been characterized by the function $b_{n,j}(\cdot)$,

TABLE I
SERVICE PARAMETERS

Parameter	Service 0	Service 1
ϵ_n	0.2	0.08
TFS_n	1	4
$Rb_{n,0}$	64 kbps	16 kbps
$\left(\frac{E_b}{N_0}\right)_{n,0}$	4.0 dB	2.5 dB
$Rb_{n,1}$	N/A	32 kbps
$\left(\frac{E_b}{N_0}\right)_{n,1}$	N/A	2.5 dB
$Rb_{n,2}$	N/A	64 kbps
$\left(\frac{E_b}{N_0}\right)_{n,2}$	N/A	2.5 dB
$Rb_{n,3}$	N/A	128 kbps
$\left(\frac{E_b}{N_0}\right)_{n,3}$	N/A	2.5 dB

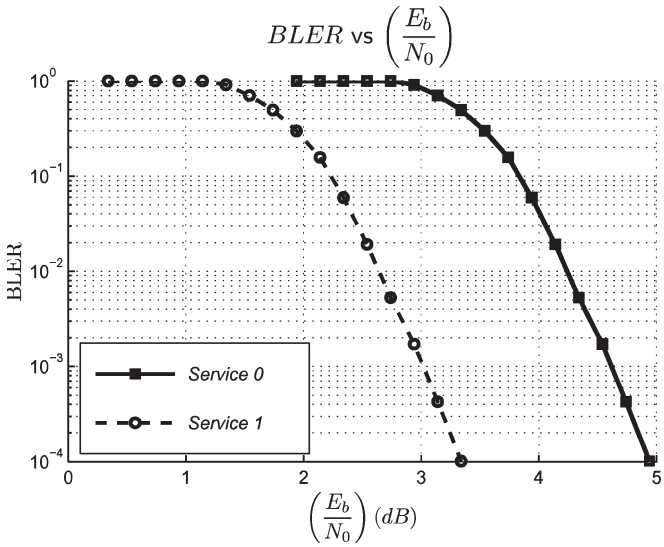

Fig. 2. Service BLER versus E_b/N_0.

as shown in Fig. 2. Notice that $\gamma_{n,j}(\cdot)$ is obtained by solving $\gamma_{n,j}(P) = b_{n,j}(g(P))$ [see (26)]. Curves shown in Fig. 2 have been obtained through a link level simulator that includes the 1500-Hz closed-loop power control, 1/3 turbo coding effect, and channel impulse response estimation.

A. Case Study 1

In the first analysis approach, a nonuniform traffic spatial distribution is considered in a single service scenario including only service 0. The scenario is composed of two traffic layers (L_0 and L_1), as shown in Fig. 3. Case study parameters are listed in Table II. It represents a hotspot region where there is a higher concentration of traffic.

Fig. 4(a) and (b) plots the pdf of the required transmitted power for different D_1 values when α_1 is varied. In both figures, a load factor $\eta = 0.8$ is considered. α_1 is varied from 0 to 1. When $\alpha_1 = 0$, there are no users within layer L_1, and thus, users are uniformly distributed all around a cell of radius r_0. On the other hand, when $\alpha_1 = 1$ all users are spread over layer L_1, whose center is placed 150 m [Fig. 4(a)] or 950 m [Fig. 4(b)] from the cell site. The distribution of the total required transmitted power is the weighted sum of the distributions of layers L_0 and L_1 components. Thus, for small

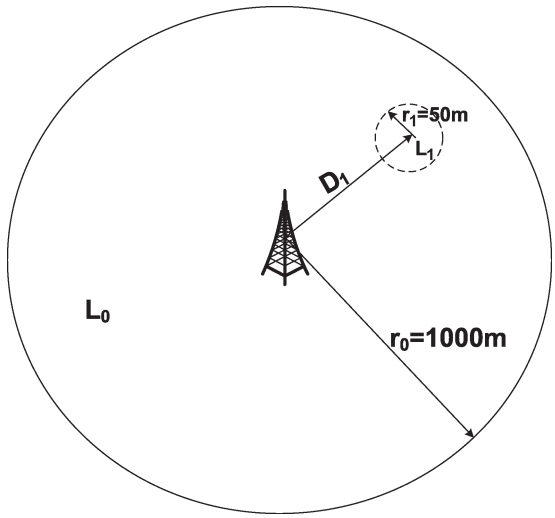

Fig. 3. Case study 1 layout.

TABLE II
CASE STUDY 1 PARAMETERS

Parameter	Value
r_0	1000 m
D_0	0 m
α_0	1-α_1
r_1	50 m
D_1	[50 m, 950 m]
α_1	[0.0, 1.0]

D_1 values two peaks arise in the total pdf (one for each layer). As distance D_1 is increased, the peak associated with layer L_1 is moved to higher values. For high D_1 values, contributions of the two layers result in a single peak [Fig. 4(b)]. For instance, when $D_1 = 150$ m, peaks are centered at about -12 and 15 dBm. If $D_1 = 950$ m, a single peak is centered at about 15 dBm. It is also remarkable that for high D_1, the single pdf peak narrows as α_1 increases because users are more concentrated spatially.

The validation of the model has been carried out through simulations. Fig. 4(c) plots a comparison between required transmitted power pdfs obtained theoretically and with simulations. It is shown that differences are minor, and the model fits the results obtained by simulation.

As transmitted power is upper bounded by P_{Tmax}, the performance of the system is tightly coupled with values over this threshold (in this particular case, 21 dBm). Fig. 5(a) and (b) shows the outage associated to case study 1. In these figures, two different situations are examined, namely 1) L_1 is close to the base station [Fig. 5(a)], and 2) L_1 is far from the base station [Fig. 5(b)]. Taking into account that outage will be lower if users are concentrated in the vicinity of the base station, in Fig. 5(a), high α_1 implies low outage probability, whereas in Fig. 5(b), high α_1 implies high outage.

The same interpretation stated for outage probability is valid for BLER. Fig. 5(c) and (d) shows the average BLER in the same conditions in which outage was obtained. The target BLER is set to 5%, which is associated with an $E_b/N_0 = 4$ dB. All results have been obtained analytically.

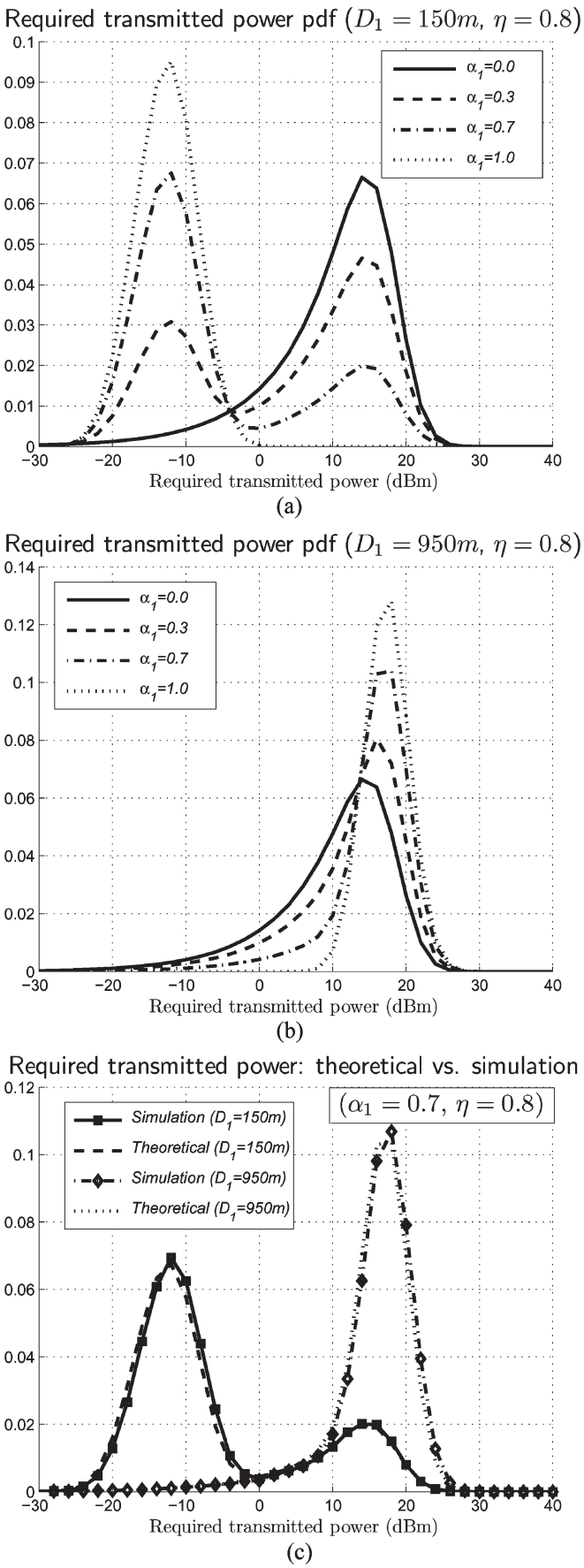

Fig. 4. Required transmitted power pdf (a) with $D_1 = 150$ m, (b) with $D_1 = 950$ m, and (c) validation of the model.

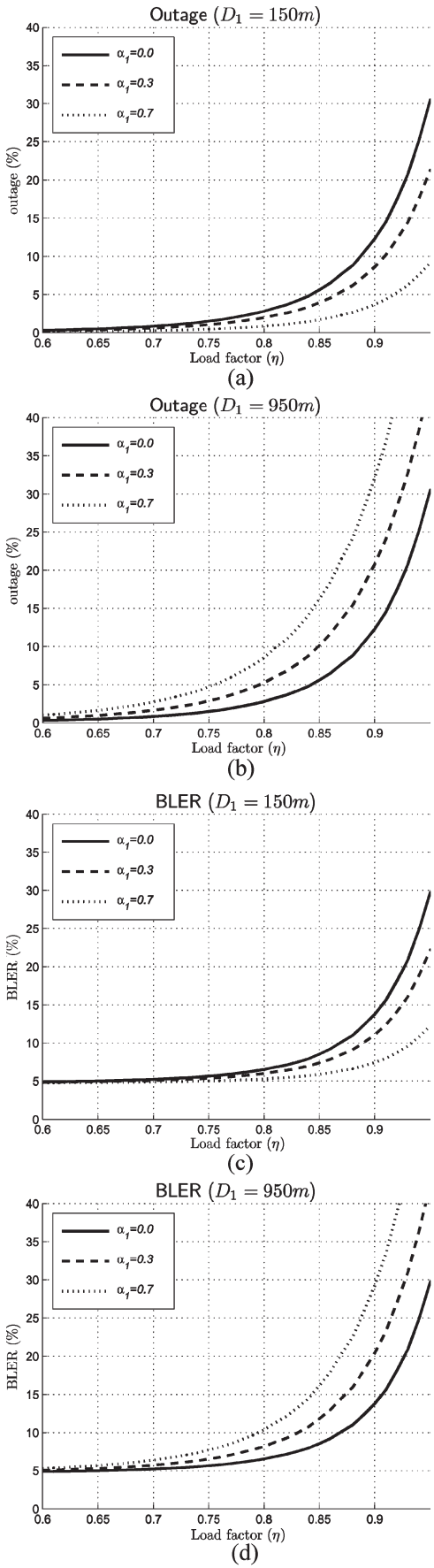

Fig. 5. Outage [with (a) $D_1 = 150$ m and (b) $D_1 = 950$ m] and BLER [with (c) $D_1 = 150$ m and (d) $D_1 = 950$ m].

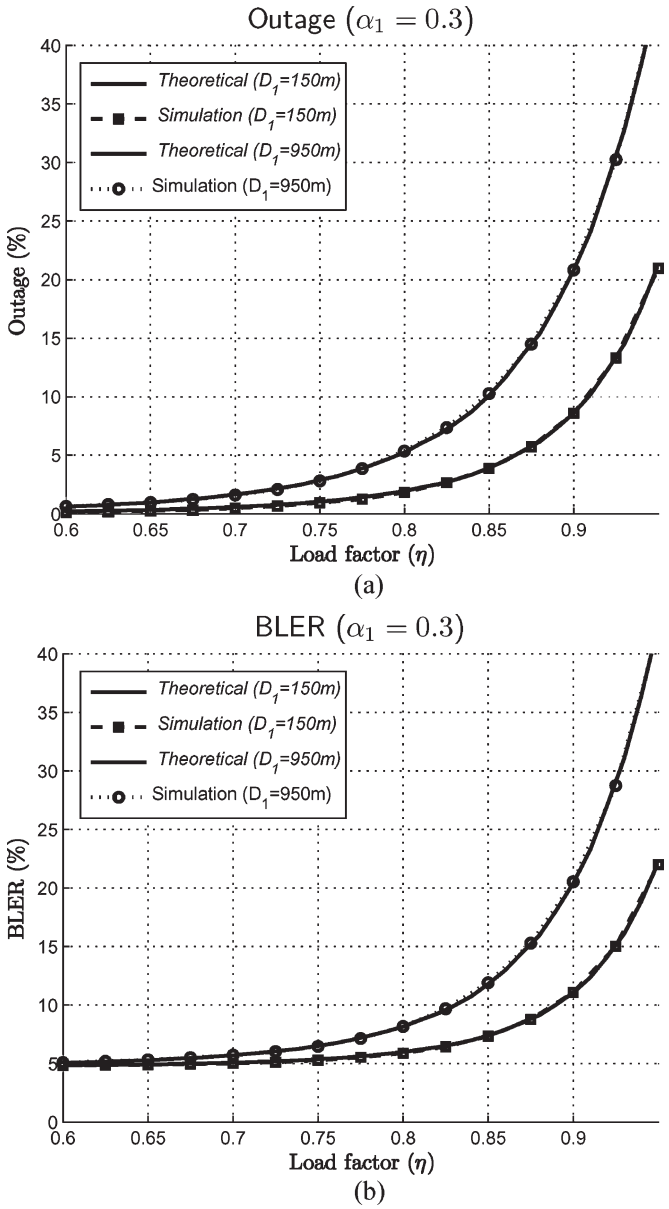

Fig. 6. Validation of (a) outage and (b) BLER with $\alpha_1 = 0.3$.

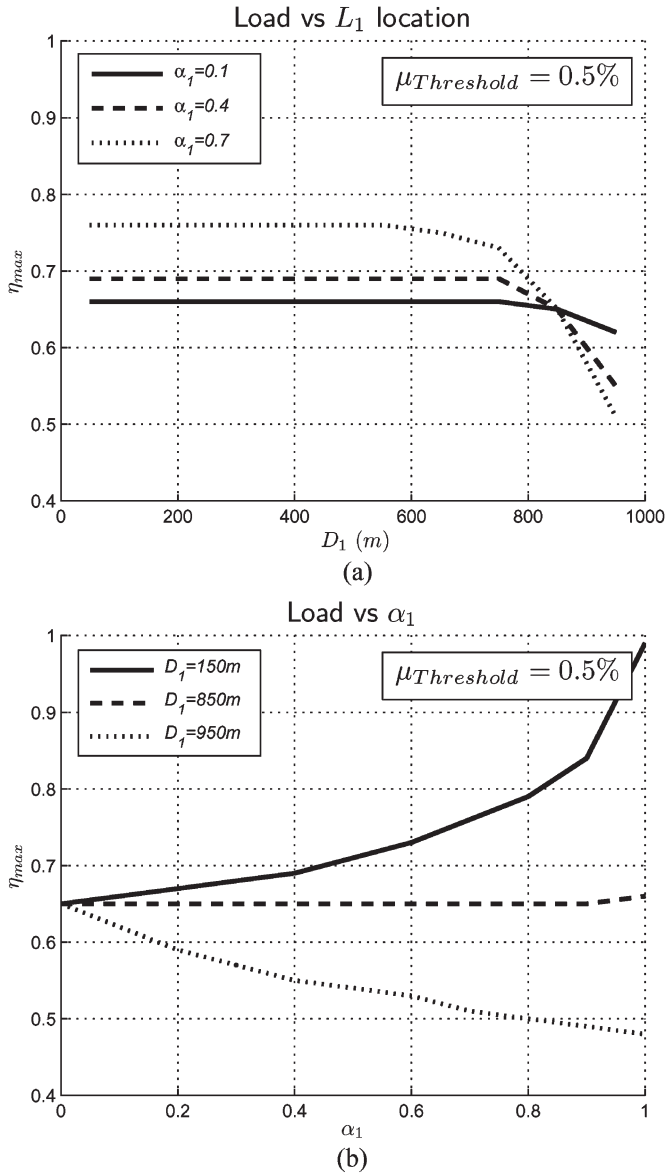

Fig. 7. Load factor corresponding to $\mu_{\text{Threshold}} = 0.5\%$ as a function of (a) D_1 and (b) α_1.

In order to validate such results, Fig. 6(a) and (b) compares the results obtained theoretically and through simulations. In both figures, α_1 has been set to 0.3 and D_1 is set to 150 or 950 m. Differences observed between simulation and theory are negligible.

If a maximum outage probability threshold $\mu_{\text{Threshold}}$ is set, it is possible to determine the maximum cell capacity, which is given by the maximum load factor level $\eta_{\max}$ that corresponds to this outage threshold. This maximum load factor level could be the input to the different uplink RRM algorithms, e.g., admission or load control. Fig. 7(a) and (b) shows the maximum allowable load factor level for an outage probability threshold $\mu_{\text{Threshold}} = 0.5\%$. The former shows the evolution of the maximum allowable load when D_1 is varied. The latter depicts the same evolution as a function of α_1. It is observed in Fig. 7(a) that high α_1 values lead to higher capacity (high load) when D_1 is small because most users are concentrated close to the base station. On the other hand, it implies a decrease of capacity as D_1 increases. Fig. 7(b) plots the same effect by varying α_1.

Note that in Fig. 7(a) outage level matches up for all cases ($\alpha_1 = 0.1$, $\alpha_1 = 0.4$, and $\alpha_1 = 0.7$) when $D_1 = 850$ m, and in fact, it could be extended to any α_1 value. This effect is due to the total loss pdfs of each layer (L_0 and L_1). When $r_0 = 1000$ m and $D_1 = 850$ m, both pdfs are centered at the same range of values. Then, the final total loss pdf does not vary significantly for different α_0 and α_1 values, assuming that only two layers are considered. As the outage probability is computed from the final pdf, the outage is similar for all α_1 values.

Three different trends may be observed in Fig. 7(b). When $D_1 = 150$ m, the maximum load factor $\eta_{\max}$ increases with α_1; when $D_1 = 850$ m, the maximum load factor remains constant; finally, when $D_1 = 950$ m, the maximum load decreases as

TABLE III
CASE STUDY 2 PARAMETERS

Parameter	Value
r_0	1000 m
D_0	0 m
α_0	0.5
r_1	50 m
D_1	150 m
α_1	0.5

TABLE IV
SERVICE DISTRIBUTION

$\rho_{i,n}$	S_0	S_1	S_2
$\rho_{0,0}$	1.0	0.5	0.0
$\rho_{0,1}$	0.0	0.5	1.0
$\rho_{1,0}$	0.0	0.5	1.0
$\rho_{1,1}$	1.0	0.5	0.0

TABLE V
SERVICE 1 TF SELECTION PROBABILITIES

$p_{n,j}$	MAC_0	MAC_1
$p_{1,0}$	0.0	0.5
$p_{1,1}$	0.0	0.5
$p_{1,2}$	0.0	0.0
$p_{1,3}$	1.0	0.0

α_1 increases. In general, high users' concentrations in L_1 are beneficial for low D_1 scenarios, whereas low concentrations in L_1 are beneficial for high D_1.

B. Case Study 2

The scenario is composed of two traffic layers (L_0 and L_1 as in case study 1) and two services (service 0 and service 1). Scenario parameters are detailed in Tables III and IV. Table IV presents the distribution of users among layers, with three different situations, which are denoted as S_0, S_1, and S_2. In the first case (S_0), all users with service 0 are scattered within layer L_0, whereas all users with service 1 remain within layer L_1. In case S_1, there is the same number of users with service 0 and service 1 in both layers (i.e., there is no service nonuniformity but traffic spatial nonuniformity). Finally, in case S_2 all users with service 0 are scattered in L_1 and users with service 1 in L_0.

The considered scenario models an urban environment where specific areas present traffic spatial and/or service nonuniformities (e.g., bus stations). Service 1 has several possible bit rates, and thus, there is a probability associated to each of the possible TFs. These probabilities depend on the user equipment MAC algorithms for TF selection [4]. As these MAC algorithms are not the purpose of this paper, two different sets of TF selection probabilities are considered and assumed to be the result of applying two algorithms that are labeled as MAC_0 and MAC_1 whose probabilities are detailed in Table V. Fig. 3 has been obtained for a definite coding scheme used in both MAC_0 and MAC_1 algorithms. Therefore, the curve plotted in Fig. 3 is used for both MAC algorithms. Whereas MAC_1 algorithm tends to select low bit transmission rates, MAC_0 selects the highest bit transmission rate, thus representing two different QoS profiles.

Let us consider the MAC_0 algorithm. Fig. 8(a) shows the required transmitted power pdf with $\eta = 0.8$. In all cases

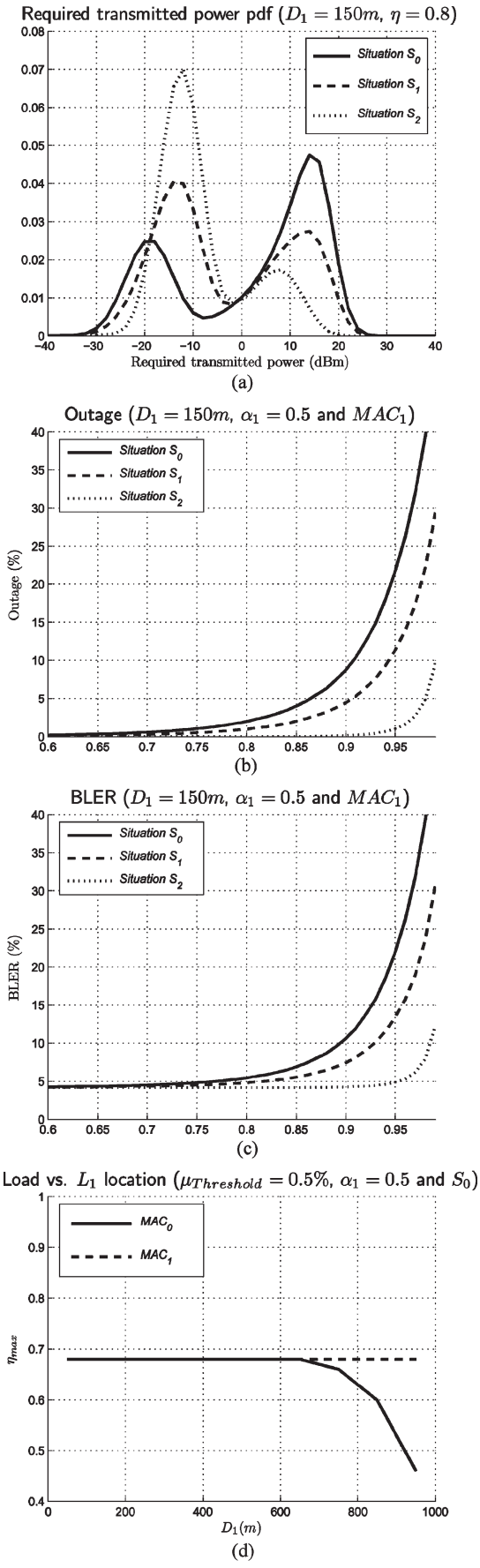

Fig. 8. (a) Required transmitted power pdf. (b) Outage. (c) BLER. (d) Load factor corresponding to $\mu_{\mathrm{Threshold}} = 0.5\%$ for MAC_0 and MAC_1.

(S_0, S_1, S_2), two peaks can be observed. Each peak is associated to one of the layers (i.e., the one appearing at low power values is associated with L_1 and the one appearing at high power values with L_0). When different services with different activity factors (ϵ_n) are mixed, the ratio between activity factors determines the proportion of users of each service. Therefore, the probability of transmitting high power levels (associated to users in layer L_0) is higher in S_0 (all users belonging to service 0 are within layer L_0) than in the others. On the other hand, when all users with service 0 are located in layer L_1 (case S_2), low transmitted power levels are more likely to occur. Finally, case S_1 presents a more balanced situation between users in each layer because, although users with service 0 have a bigger impact on transmitted power, the proportion of users with each service is maintained equal in both layers.

The previous explanation can be generalized to any load factor level. However, the higher the load factor is, the higher the required power level will be, thus increasing the outage. This effect is shown in Fig. 8(b), which plots the performance of the system in terms of outage as a function of load factor. BLER is shown in Fig. 8(c). The target BLER is set to 5% for service 0 and to 2.5% for service 1.

The impact of the two MAC algorithms and their associated TF probabilities in terms of system capacity is analyzed in Fig. 8(d). The outage threshold is set to 0.5% in S_0. Notice that differences arise for high D_1 values. In fact, results obtained with different MAC strategies are more significant as differences in used $(E_b/N_0) \cdot R_b$ increase. Fig. 8(d) plots a comparison between the two algorithms detailed in Table V as a function of D_1. In this case, the capacity is reduced when high transmission bit rates are more likely to be selected (MAC_0). The capacity in terms of load factor is maintained for the whole range of D_1 with MAC_1 because selected transmission bit rates are low and do not imply an increase of the outage even for high D_1. When MAC_0 is used, the selection of high transmission bit rate causes an increase on outage, and thus, the capacity is reduced.

C. Case Study 3

In this section, an example of a more complex scenario is analyzed (Fig. 9). The scenario is now composed of four traffic layers and the same two services used in case study 2 (Table I). Parameters are shown in Tables VI and VII. In the first layer (L_0), there are only users with service 0. Three nonuniformities are placed within the cell (layers L_1, L_2, and L_3), in which only users with service 1 are considered. Service 1 uses the MAC_1 algorithm detailed in Table V.

In previous case studies, the interpretation of the concrete results obtained with the derived expressions was not difficult to be carried out due to the reduced number of services and layers under study. However, as the number of layers and/or services increases, the interpretation becomes less obvious. Therefore, in such case studies, the proposed analytical model becomes a suitable tool to evaluate the cell capacity. Case study 3 intends to show an example of these complex scenarios. Fig. 10(a) plots the required transmitted power pdf where all effects of traffic spatial and service distributions are mixed up.

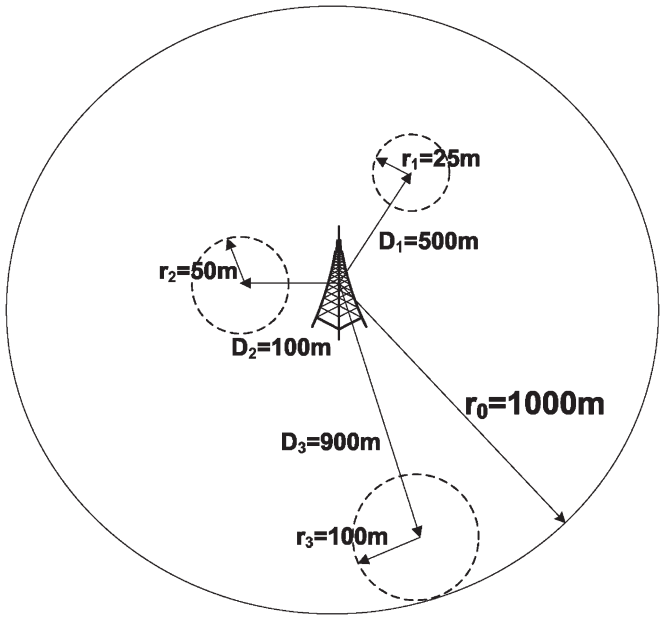

Fig. 9. Case study 3 layout.

TABLE VI
CASE STUDY 3 PARAMETERS

Parameter	Value
r_0	1000 m
D_0	0 m
α_0	0.4
r_1	25 m
D_1	500 m
α_1	0.2
r_2	50 m
D_2	100 m
α_2	0.2
r_3	100 m
D_3	900 m
α_3	0.2

TABLE VII
SERVICE DISTRIBUTION

Parameter	Value
$\rho_{0,0}$	1.0
$\rho_{0,1}$	0.0
$\rho_{1,0}$	0.0
$\rho_{1,1}$	1.0
$\rho_{2,0}$	0.0
$\rho_{2,1}$	1.0
$\rho_{3,0}$	0.0
$\rho_{3,1}$	1.0

Fig. 10(b) shows the total, service 0, and service 1 outage probabilities. Users with service 1 present the best performance in terms of outage probability due to the distance at which L_1 and L_2 layers are located. Sixty percent of the users use service 1. Two out of three users with service 1 belong to layer L_1 or L_2. As L_1 and L_2 have their center at 500 and 100 m, respectively, and their radii are 25 and 50 m, there are no users of layers L_1 and L_2 at a distance higher than 525 m. Forty percent of the users use service 0 and are spread in layer L_0, whose radius is 1000 m. Therefore, outage of users with service 1 is lower than that of users with service 0. Finally, the total outage is the sum of the contribution of both services.

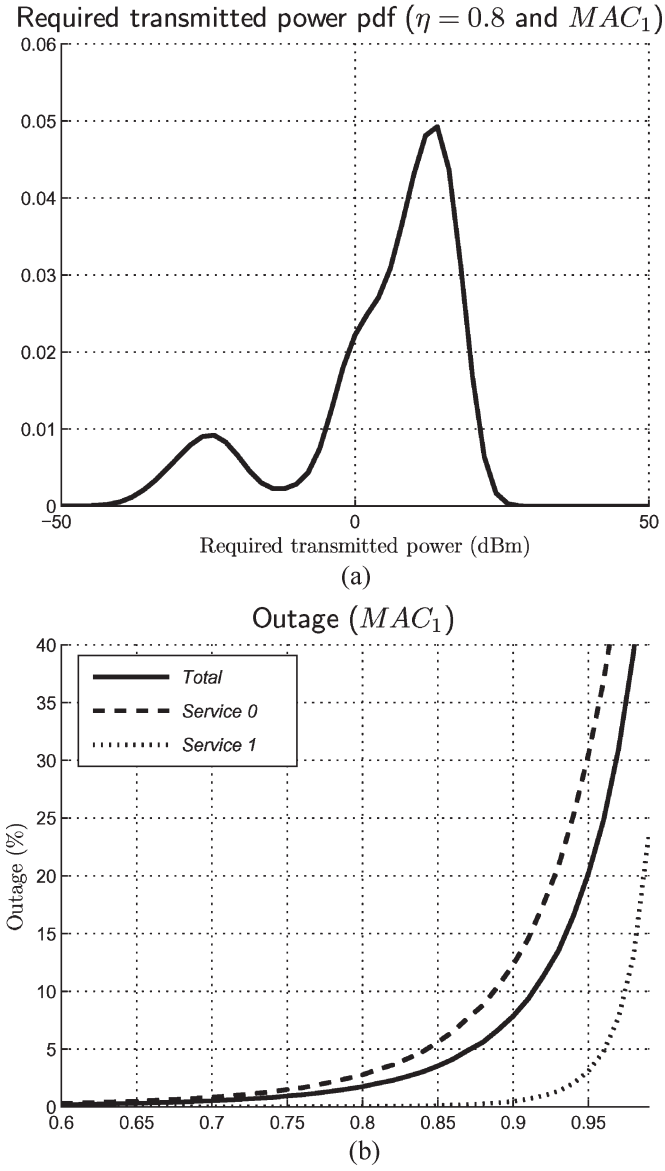

Fig. 10. (a) Required transmitted power. (b) Total, service 0, and service 1 outage probabilities for case study 3.

Despite having 60% of the users using service 1 and only 40% using service 0, the total outage curve is close to the curve of service 0 because of the higher activity factor of service 0. In particular, if the threshold outage $\eta_{\text{Threshold}}$ is set to 0.5%, the maximum load factor for case study 3 is 0.69.

V. Conclusion

An analytical model has been proposed for the reverse link of a WCDMA system with traffic nonuniform distribution and supporting multiple services. The main contribution of the article lies on the generalization of hotspots in terms of spatial traffic nonuniformities as well as in terms of service distribution nonuniformities. QoS parameters, such as BLER and outage probability, have been characterized for a circular cell with circular nonuniformities or hotspots, though the description of the process may also be applied to any known scenario by properly replacing the path loss pdfs. Therefore, the proposed model allows a detailed study of the impact caused by the mix of different services in a nonuniformly distributed scenario and the computation of the maximum capacity (i.e., the maximum uplink load factor that can be supported for specific QoS constraints). A proper maximum load selection becomes a key point to maximize the capacity, whereas average outage or BLER probabilities are maintained below a design value. An excessively high load threshold could degrade the performance of the system. On the other hand, too low loads would not be efficient in terms of available resources usage. Some case studies have been analyzed, and the maximum load factor has been obtained.

Different conclusions have been highlighted in the analyzed case studies. In particular, it has been observed that the maximum admissible load factor $\eta_{\max}$ is dependent on the traffic distribution, which is characterized in this paper through the number of traffic layers and the location and the proportion of traffic in each layer. The variability of $\eta_{\max}$ is shown to be higher when hotspots are located either in the vicinity of the base station or close to the cell border, whereas it presents a more stable behavior for intermediate locations. Likewise, MAC algorithms have an important impact on the capacity of the system, and those MAC algorithms that use high transmission bit rates lead to lower maximum load factors.

Finally, the complexity to determine the maximum load factor increases as the number of layers and/or services is increased. The potentials of the model are stressed in these scenarios, where the prediction of the load values is to be used as RRM algorithm input. In particular, one of the most important RRM strategies is the CAC. This procedure is usually carried out by setting a maximum allowable load factor $\eta_{\max}$, which is used to decide whether a new connection should be admitted or rejected. Usually, this maximum load is determined regardless of the traffic distribution. It has been demonstrated throughout this paper that in scenarios with traffic nonhomogeneities this value varies. The maximum allowable load factor can be easily obtained in simple scenarios. However, as the complexity of the scenario increases, it becomes more and more difficult to predict $\eta_{\max}$; thus, the proposed methodology becomes a useful tool.

Appendix

In the following, the pdf of the path loss of a traffic layer, as defined in Section II, is computed. As shown in (6), the path loss is dependent on the distance to the base station (d). Then, the first step to obtain the pdf of the path loss $(f_Y(y))$ is the calculation of the distance pdf $(f_D(d))$ of a generic round-shaped layer i with radius r_i (in meters) and whose center is placed D_i meters from the coordinate origin. The distance probability distribution function presents two different cases.

Case 1—$D_i < r_i$: If $D_i < r_i$, the distance probability distribution function of layer L_i is defined as

$$F_D^i(d) = prob(d \le D) = \frac{A_{\text{TOT}}}{\pi r_i^2} \tag{34}$$

where A_{TOT} is the layer L_i area intersected with a circle of radius d, as shown in Fig. 11. Notice that $A_{\text{TOT}} = \pi d^2$ when

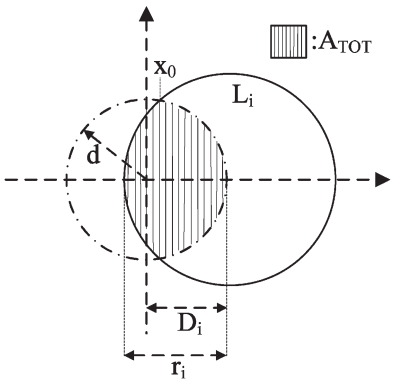

Fig. 11. Scheme of the situation when $D_i < r_i$ and $d > r_i - D_i$.

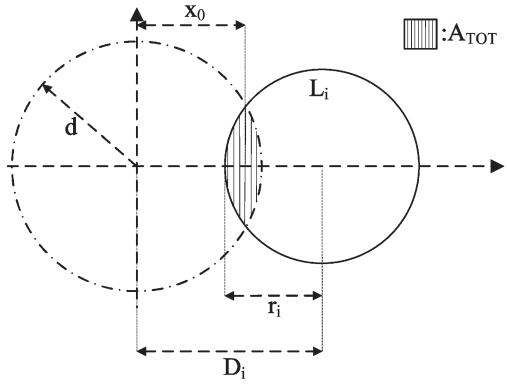

Fig. 12. Location of the generic layer when $D_i \geq r_i$.

$d \leq r_i - D_i$ (i.e., the circle of radius d is inside the circle of radius r_i). However, when $d > r_i - D_i$, A_{TOT} is given as follows (see Fig. 11):

$$A_{\mathrm{TOT}} = 2\int_{D_i - r_i}^{x_0} \sqrt{(r_i^2 - (x - D_i)^2)}dx + 2\int_{x_0}^{d} \sqrt{(d^2 - x^2)}dx \tag{35}$$

where

$$x_0 = \frac{D_i^2 + d^2 - r_i^2}{2D_i} \tag{36}$$

as shown in Fig. 11. By computation, we have

$$\begin{aligned} A_{\mathrm{TOT}} = {} & \frac{\pi}{2}\left(d^2 + r_i^2\right) - d\arcsin\left(\frac{D_i + d^2 - r_i^2}{2dD_i}\right) \\ & + r_i^2 \arcsin\left(\frac{d^2 - D_i - r_i^2}{2r_i D_i}\right) \\ & - \frac{1}{2}\sqrt{(d^2 - (D_i - r_i)^2)}\left((D_i - r_i)^2 - d^2\right). \end{aligned} \tag{37}$$

Therefore, substituting (37) in (34) yields

$$F_D^i(d) = \frac{d^2}{r_i^2} \tag{38}$$

if $0 \leq d \leq (r_i - D_i)$, or

$$\begin{aligned} F_D^i(d) = \frac{1}{\pi r_i^2}\Bigg[& \frac{\pi}{2}\left(d^2 + r_i^2\right) - d^2\arcsin\left(\frac{D_i^2 + d^2 - r_i^2}{2D_i d}\right) \\ & + r_i^2 \arcsin\left(\frac{d^2 - D_i^2 - r_i^2}{2D_i r_i}\right) \\ & - \frac{1}{2}\sqrt{(d^2 - (D_i - r_i)^2)\left((D_i + r_i)^2 - d^2\right)}\Bigg] \end{aligned} \tag{39}$$

if $(r_i - D_i) \leq d \leq (D_i + r_i)$.

The pdf is obtained by deriving (38) and (39) as a function of distance d, i.e.,

$$f_D^i(d) = \frac{2d}{r_i^2} \tag{40}$$

in the range $0 \leq d \leq (r_i - D_i)$, and

$$f_D^i(d) = \frac{1}{\pi r_i^2}\left[\pi d - 2d\arcsin\left(\frac{D_i^2 + d^2 - r_i^2}{2D_i d}\right)\right] \tag{41}$$

in the range $(r_i - D_i) \leq d \leq (D_i + r_i)$.

Case 2—$D_i \geq r_i$: If $D_i \geq r_i$ (Fig. 12), A_{TOT} is analogous to the case obtained in (37), and thus, the probability distribution function is expressed as

$$\begin{aligned} F_D^i(d) = \frac{1}{\pi r_i^2}\Bigg[& \frac{\pi}{2}\left(d^2 + r_i^2\right) - d^2\arcsin\left(\frac{D_i^2 + d^2 - r_i^2}{2D_i d}\right) \\ & + r_i^2 \arcsin\left(\frac{d^2 - D_i^2 - r_i^2}{2D_i r_i}\right) \\ & - \frac{1}{2}\sqrt{(d^2 - (D_i - r_i)^2)\left((D_i + r_i)^2 - d^2\right)}\Bigg] \end{aligned} \tag{42}$$

in the range $(D_i - r_i) \leq d \leq (D_i + r_i)$.

Therefore, the pdf is given as follows:

$$f_D^i(d) = \frac{1}{\pi r_i^2}\left[\pi d - 2d\arcsin\left(\frac{D_i^2 + d^2 - r_i^2}{2D_i d}\right)\right] \tag{43}$$

in the range $(D_i - r_i) \leq d \leq (D_i + r_i)$.

Once distance distribution is obtained, path loss distribution may be calculated through the relationship existing between distance d and path loss Y extracted from (6). In linear units, distance is expressed as follows:

$$d = 10^{\frac{Y - Y_0}{\zeta}} = g^{-1}(Y). \tag{44}$$

In this context, $f_Y(y)$ can be obtained from $f_D(d)$. Since d is a continuous random variable and $g^{-1}(Y)$ is a differentiable

function, $f_Y(y)$ is given by

$$f_Y^i(y) = f_D^i\left(g^{-1}(y)\right)\left|\frac{dg^{-1}(y)}{dy}\right|. \quad (45)$$

Then, introducing (40), (41), (43), and (44) in (45), it finally yields the pdf of the propagation loss given in (7)–(9).

ACKNOWLEDGMENT

This work was performed in the framework of the Project IST-AROMA (http://www.aroma-ist.upc.edu).

REFERENCES

[1] R. Ganesh and K. Joseph, "Effect of non-uniform traffic distributions on performance of a cellular CDMA system," in *Proc. IEEE ICUPC*, San Diego, CA, Oct. 1997, pp. 598–602.
[2] B. O. Adrian, S. G. Haggman, and A. Pietila, "Study of the impact of non-uniform spatial traffic distribution on the system parameters of CDMA cellular networks," in *Proc. IEEE ICPWC*, Jaipur, India, Feb. 1999, pp. 394–398.
[3] F. Adelantado, O. Sallent, J. Pérez-Romero, and R. Agustí, "Impact of traffic hotspots in 3G W-CDMA networks," in *Proc. IEEE VTC—Spring*, Milan, Italia, May 2004, pp. 2332–2336.
[4] J. Pérez-Romero, O. Sallent, R. Agustí, and M. A. Díaz-Guerra, *Radio Resource Management Strategies in UMTS*. Hoboken, NJ: Wiley, 2005.
[5] I. Koo, S. Bahng, and K. Kim, "Resource reservation in call admission control schemes for CDMA system with non-uniform traffic distribution among cells," in *Proc. IEEE VTC—Spring*, Jeju Island, Korea, Apr. 2003, pp. 438–441.
[6] J. H. Kim, H. J. Yeo, H. Park, and Y. K. Jhee, "Hybrid call admission control scheme supporting voice/video/packet data services with W-CDMA downlink power allocation," in *Proc. IEEE VTC—Spring*, Milan, Italy, May 2004, pp. 2753–2757.
[7] H. Zhu, T. Buot, R. Nagaike, and S. Harmen, "Load balancing in WCDMA systems by adjusting pilot power," in *Proc. IEEE ICPWC*, New Delhi, India, Dec. 2002, pp. 936–940.
[8] K. Valkealahti, A. Hoglund, J. Parkkinen, and A. Flanagan, "WCDMA common pilot power control with cost function minimization," in *Proc. IEEE VTC—Fall*, Vancouver, BC, Canada, Sep. 2002, pp. 2244–2247.
[9] I. Siomina and D. Yuan, "Optimization of pilot power for load balancing in WCDMA networks," in *Proc. IEEE GLOBECOM Conf.*, Dallas, TX, Nov. 2004, pp. 3872–3876.
[10] M. Subramaniam and A. Anpalagan, "A pilot power based power control (PPBPC) and base station assignment algorithm in cellular CDMA networks," in *Proc. CCECE*, Niagara Falls, ON, Canada, May 2004, pp. 327–333.
[11] F. Adelantado and F. Casadevall, "Dynamic common pilot power management in a real hot spot environment," in *Proc. IEEE GLOBECOM Conf.*, St. Louis, MO, Nov. 2005, pp. 3529–3533.
[12] H. Holma and A. Toskala, *WCDMA for UMTS*. Hoboken, NJ: Wiley, 2004.
[13] "Multiplexing and channel coding (fdd)," Tech. Rep. TS 25.212, Sep. 2005. 3GPP, v6.6.0.

Ferran Adelantado (S'01) was born in Barcelona, Spain, in 1978. He received the M.Sc. degree in telecommunications engineering from the Universitat Politècnica de Catalunya (UPC), Barcelona, in 2001. He is currently working toward the Ph.D. degree with the Department of Signal Theory and Communications, UPC, through a grant from the Spanish Ministry of Science and Technology.

He has been involved in European projects as well as in a project for a private company. His research interests include MAC protocols and RRM techniques for wireless communication systems, particularly systems with radio interfaces based on WCDMA.

Jordi Pérez-Romero (M'04) was born in Barcelona, Spain, in 1974. He received the M.Sc. degree in telecommunications engineering and the Ph.D. degree from the Universitat Politècnica de Catalunya (UPC), Barcelona, in 1997 and 2001, respectively.

In January 1998, he joined the Radio Communications Group, through a grant from the Spanish Educational Ministry. He is currently an Associate Professor with UPC. His research interests are in the field of mobile communication systems, particularly packet radio techniques, spread-spectrum systems, radio resource and QoS management, and heterogeneous wireless networks. He has been involved in different European Projects (e.g., WINEGLASS, ARROWS, EVEREST, E2R, NEWCOM, and AROMA) as well as in projects for private companies such as Telefónica and Alcatel. He has published several papers in IEEE journals and conference proceedings. He has also published the book *Radio Resource Management Strategies in UMTS* (Wiley, 2005).

Oriol Sallent received the M.Sc. degree in telecommunications engineering and the Ph.D. degree from the Universitat Politècnica de Catalunya (UPC), Barcelona, Spain, in 1994 and 1997, respectively.

He is an Associate Professor with the UPC. His research interests are in the field of radio resource and spectrum management for heterogeneous cognitive wireless networks, where he has published a number of papers in IEEE journals and conference proceedings. He has participated in many research projects and consultancies funded by either public organizations or private companies. He is currently participating in the projects IST-E2R2 and IST-AROMA.